

# Exposing nontrivial flat bands and superconducting pairing in infinite-layer nickelates

Ruiqi Zhang,<sup>1</sup> Cheng-Yi Huang,<sup>2</sup> Mehdi Kargarian,<sup>3</sup> Rahul Verma,<sup>4</sup> Robert S. Markiewicz,<sup>2</sup> Arun Bansil,<sup>2</sup> Jianwei Sun,<sup>1,\*</sup> and Bahadur Singh<sup>4,†</sup>

<sup>1</sup>*Department of Physics and Engineering Physics,  
Tulane University, New Orleans, LA 70118, USA*

<sup>2</sup>*Department of Physics, Northeastern University, Boston, MA 02115, USA*

<sup>3</sup>*Department of Physics, Sharif University of Technology, Tehran, Iran*

<sup>4</sup>*Department of Condensed Matter Physics and Materials Science,  
Tata Institute of Fundamental Research, Mumbai 400005, India*

Flat bands coupled with magnetism and topological orders near or at the Fermi level are well known to drive exotic correlation physics and unconventional superconductivity. Here, based on first-principles modeling combined with an in-depth symmetry analysis, we reveal the presence of topological flat bands involving low-energy Ni- $3d_{z^2}$  states in the recently discovered superconductor LaNiO<sub>2</sub>. Our analysis demonstrates that LaNiO<sub>2</sub> is an Axion insulator with  $\mathbb{Z}_4 = 2$  and that it supports topological crystalline insulating states protected by the glide mirror symmetries. The topological flat bands in LaNiO<sub>2</sub> are also shown to host odd-parity superconductivity. Our study indicates that the nickelates would provide an interesting materials platform for exploring the interplay of flat bands, topological states, and superconductivity.

*Introduction.* Flat bands in quantum materials provide a robust basis for investigating many-body physics, including non-Fermi liquids and unconventional superconductivity interwoven with nontrivial electronic states [1–6]. Suppression of electronic kinetic energy in a flat band produces electron localization in real space and the emergence of highly degenerate electronic states. Although models and materials have been proposed [4, 5], the experimental realization of flat bands has been limited mainly to moiré lattice materials such as twisted bilayer graphene (TBLG) and kagome materials [3, 6]. The mechanism in moiré materials involves the flattening of the Dirac cone dispersion through spatial variations of the interlayer coupling that restructures the underlying lattice and yields a smaller Brillouin zone [7]. The moiré materials although exhibit nontrivial states coexisting with superconducting, magnetic, and other correlated states, but controlling their properties requires complex tuning of structural parameters. For this reason, stoichiometric crystals with flat bands are more appealing for exploring the physics of high electron density coupled with nontrivial topology [1–3], and the kagome materials are drawing intense current interest [3, 8–13]. However, the flat bands in the kagome materials usually lie away from the Fermi level [3], and therefore, it is not clear how these bands participate in driving superconductivity. It is important therefore to find superconducting materials that support low-energy flat bands that coexist with other correlated states [1–3].

The cuprates have been shown recently to host high-order van Hove singularities (VHSs) and flat bands which could drive correlated phases such as superconductivity and supermetals [14]. Here we characterize the topo-

logical flat bands and superconducting pairing symmetries of the recently discovered infinite-layer (IL) nickelate superconductors that have emerged as a promising analog of the cuprates [15–21]. Extensive experimental and theoretical efforts have been devoted to finding similarities and differences between the infinite-layer (IL) nickelates and the cuprates [22–37]. For instance, competing charge orders [38–40], superconductivity [38, 41], and magnetism [42, 43] has been reported recently in the *undoped* IL-nickelates [15, 43, 44]. These findings sharply contrast with the *undoped* cuprates, which host a well-defined AFM ground state. The pairing symmetry in IL-nickelates, however, remains unclear [30, 45–47]. Although the participation of Ni  $3d_{z^2}$ -like flat bands in superconducting pairing is indicated [48], their topological character and the associated pairing symmetries have not been identified [49].

In this Letter, we unveil the presence of topological flat bands in the parent nickelate superconductor LaNiO<sub>2</sub> and discuss the associated pairing symmetries. LaNiO<sub>2</sub> has been shown to support various low-energy competing magnetic phases with *C*-type antiferromagnetic (*C*-AFM) ground state [35, 36]. The *C*-AFM state supports flat bands primarily composed of Ni  $3d_{z^2}$  states with VHSs at the Fermi level, which would enhance many-body interactions and drive exotic correlated phenomena [35, 50]. We delineate the topological character of LaNiO<sub>2</sub> and its nontrivial topological state. Our in-depth symmetry analysis of the bulk bands and surface states shows that the *C*-AFM phase realizes an axion insulator state with  $\mathbb{Z}_4 = 2$  and a glide-mirror-symmetry protected topological crystalline insulating (TCI) state. We also characterize the superconducting pairing symmetries associated with the bulk flat bands at the Fermi level and discuss the possibility of an odd-parity pairing in LaNiO<sub>2</sub>. Our study indicates that LaNiO<sub>2</sub> is a materials promising platform for exploring the interplay of topological flat bands and unconventional superconductivity.

\* Corresponding author: [jsun@tulane.edu](mailto:jsun@tulane.edu)

† Corresponding author: [bahadur.singh@tifr.res.in](mailto:bahadur.singh@tifr.res.in)

tivity.

*Methods.* All calculations were performed by using the projector-augmented wave method [51] as implemented in the Vienna *ab initio* simulation package (VASP) [52, 53]. A high-energy cutoff of 520 eV was used to truncate the plane-wave basis set. The exchange-correlation effects were treated using the strongly constrained and appropriately normed (SCAN) density functional without any adjustable parameters [54]. The crystal structures and ionic positions were fully optimized using a force convergence criterion of 0.01 eV/Å for each atom along with a total energy tolerance of  $10^{-6}$  eV. Notably, substantial recent studies have shown the efficacy of SCAN for accurately modeling ground states and electronic structure of strongly correlated systems such as the cuprates [55–57] and nickelates [35, 36], binary 3d oxides [58], and especially the *f*-electron system SmB<sub>6</sub> [59] due to the reduction of self-interaction error in comparison with other widely used density functionals [58]. We adopted a  $16 \times 16 \times 16$   $\Gamma$ -centered  $k$  mesh to sample the primitive bulk Brillouin zone (BZ) and total energy calculations. Spin-orbit coupling (SOC) effects were included self-consistently. Topological properties were calculated by generating a material-specific tight-binding model Hamiltonian using the VASP2WANNIER90 interface [60]. La *f* and *d*, Ni *d*, and O *p* states were included for constructing the Wannier functions. The surface spectral weight of semi-infinite slabs was calculated using an iterative Green’s function method [61, 62].

*Crystal structure and electronic properties.* The parent nonmagnetic LaNiO<sub>2</sub> crystallizes in the tetragonal Bravais lattice with space group  $P4/mmm$  (#123,  $D_{4h}$ ). The La, Ni, and O atoms occupy Wyckoff positions  $1d : \{\frac{1}{2}, \frac{1}{2}, \frac{1}{2}\}$ ,  $1a : \{0, 0, 0\}$ , and  $2f : \{\frac{1}{2}, 0, 0\}$ , respectively, in the lattice. The magnetic unit cell of *C*–AFM phase is constructed considering a  $\sqrt{2} \times \sqrt{2} \times 1$  supercell of nonmagnetic LaNiO<sub>2</sub> (see Fig. 1(a)). In the *C*–AFM phase, the magnetic moments of Ni atoms are aligned parallel to the tetragonal *c* axis as illustrated in Fig. 1(b). Particularly, the magnetic interaction of Ni atoms is antiferromagnetic in the plane whereas it is ferromagnetic in the out-of-plane direction. The calculated magnetic moment of Ni is  $\sim 1 \mu_B$ , which is consistent with previous DFT+*U* [50] and DMFT calculations [27]. Note that despite the absence of long-range orders in LaNiO<sub>2</sub> even at low temperatures, experiments reported the presence of local magnetic moments on Ni atoms and strong AFM interactions with competing charge orders in nickelates [42, 43]. In this context, our recent study has discovered a variety of low-energy competing magnetic phases of LaNiO<sub>2</sub> with *C*–AFM phase as the lowest energy state [35, 36]. We thus focus on the symmetry properties and topological properties of the *C*–AFM phase. It retains the  $D_{4h}$  point-group symmetry of the parent phase when the SOC effects are included. It contains 16 symmetry operations including an inversion  $\mathcal{I}$  symmetry and glide-mirror  $\mathcal{G}_v = \{\mathcal{M}_v | \frac{1}{2} \frac{1}{2} 0\}$  symmetries highlighted in Fig. 1(b). Figure 1(c) shows the first BZ of the

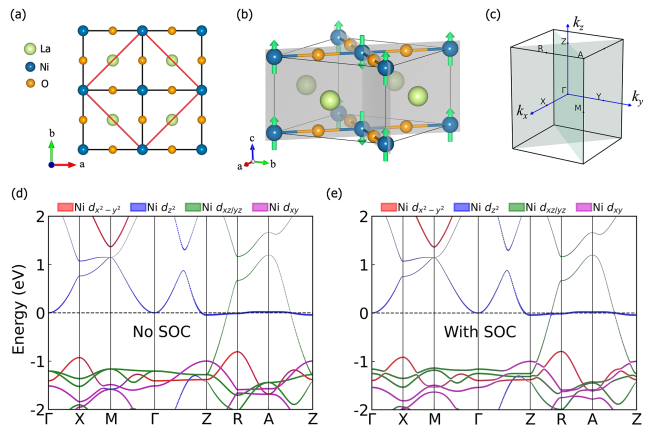


FIG. 1. (a) A  $2 \times 2$  representation of parent nonmagnetic structure of LaNiO<sub>2</sub> with the *C*–AFM unit cell marked in red color. Green, blue, and yellow balls represent La, Ni, and O atoms, respectively. (b) The perspective view of the *C*–AFM phase of LaNiO<sub>2</sub>, where  $\mathcal{M}_{110}$  and  $\mathcal{M}_{\bar{1}\bar{1}0}$  planes are highlighted. The green arrows denote magnetic moment directions. (c) The first Brillouin zone (BZ) of *C*–AFM with relevant high-symmetry points. The  $\mathcal{M}_{110}$  and  $\mathcal{M}_{\bar{1}\bar{1}0}$  planes are also shown. (d)–(e) Calculated bulk band structure of the *C*–AFM phase of LaNiO<sub>2</sub> (d) without and (e) with spin-orbit coupling. The orbital decompositions to various states are identified.

*C*–AFM phase with various high-symmetry points.

The bulk band structure of the *C*–AFM phase without SOC is shown in Fig. 1(d). A pronounced antiferromagnetic splitting of  $\sim 2$  eV in Ni  $3d_{x^2-y^2}$  bands is evident in accord with earlier DFT+*U* [50] and experimental studies [40]. More importantly, we observe the presence of a nearly flat band pinned precisely at the Fermi level on the  $k_z = \pi/c$  plane. This flat band intersects with another itinerant band to form nodal band crossings along the  $Z$ – $R$  and  $A$ – $Z$  high-symmetry directions. The detailed orbital analysis shows that the flat band is predominantly composed of Ni  $3d_{z^2}$  orbitals and crosses with O  $2p$  and Ni  $3d_{xz/yz}$  derived itinerant band to form a nodal band crossing. Upon considering the SOC effects in Fig. 1(e), a minuscule gap opens up these crossing points, forming a continuous local band gap between the valence and conduction bands.

*Flat band and the nontrivial topological state.* To characterize the flat band and nontrivial state, we present the close-up of the band structure without and with SOC in Figs. 2(a) and 2(b), respectively. Interestingly, a scan of the nodal crossings in the full BZ unfolds a nearly dispersionless nodal line on the  $k_z = \pi/c$  plane without SOC as illustrated in the inset of Fig. 2(a). The inclusion of SOC drives an inverted insulating gap of  $\leq 5$  meV between band-1 and band-2 in Fig. 2(b). For clarity, we denote the two intersecting bands at the Fermi level as band-1 and band-2 in Fig. 2(b). Band-1 primarily arises due to strong hybridization between the Ni  $3d$  and O  $2p$  orbitals (Fig. 2(f)), whereas band-2 exhibits Ni

$3d_{z^2}$  and La  $5d$  states as shown in Fig. 2(g). These findings not only infer a nontrivial character of the  $C$ -AFM phase but also underscore the necessity of a multiband model to accurately describe the low-energy physics in nickelates. We present a three-dimensional ( $E - k_x - k_y$ ) rendition of the band structure near the Fermi level in Fig. 2(d). It highlights the nearly isotropic nature of the flat bands at the  $k_z = \pi/c$  plane. Such a flat band drives high-order Van Hove singularities (VHSs) in the density of states (Fig. 2(e)) similar to *high*- $T_c$  cuprates superconductors [14]. The presence of flat bands and VHSs at the Fermi level can introduce competition among various lattice-distorted and correlated electronic states in nickelates as found in experiments. To determine the origin of the flat bands, we plot the charge density of band-1 and band-2 in Figs. 2(f)-2(g), and 2(h)-2(i). We find a power-law decay of Ni wavefunctions on the  $k_z = \pi/c$  plane, which results in highly restricted in-plane hopping between Ni spins. In contrast, the out-of-plane Ni wavefunctions are less localized, giving rise to bands with notable dispersion. This scenario aligns with Hund's coupling rules, signifying that in-plane hopping terms are significantly suppressed due to the conservation of spin while hopping along the  $c$ -axis is free from such a constraint.

The presence of an inverted band gap between band-1 and band-2 in the  $C$ -AFM phase of  $\text{LaNiO}_2$  hints towards a topological nontrivial state. To reveal the nontrivial band character, we compute the parity-based higher-order  $\mathbb{Z}_4$  invariant which is given as

$$\mathbb{Z}_4 = \sum_{i=1}^8 \sum_{n=1}^{n_{occ}} \frac{1 + \xi_n(\Lambda_i)}{2} \pmod{4} \quad (1)$$

where  $\xi_n$  is the parity eigenvalue ( $\xi_n = \pm 1$ ) of  $n^{\text{th}}$  band at time-reversal invariant momentum point  $\Lambda_i$ . The  $\mathbb{Z}_4$  is well defined even for a magnetic material preserving inversion symmetry. A centrosymmetric insulator with  $\mathbb{Z}_4 = 2$  indicates an axion insulator state with a quantized topological magnetoelectric effect with axion coupling  $\theta = \pi$  [63]. Based on the parity eigenvalues of occupied states, we obtained  $\mathbb{Z}_4$  of 2, which demonstrates that the  $C$ -AFM phase of  $\text{LaNiO}_2$  is an antiferromagnetic axion insulator. It can support the half-quantized quantum Hall effect if the associated surface states are gapped.

Since the system respects  $\mathcal{G}_{v_1} = \{\mathcal{M}_{v_1} | \frac{1}{2}\frac{1}{2}0\}$ , we also evaluated the mirror Chern number on the  $k_x = k_y$  plane. The evolution of the Wannier charge centers (WCCs) associated with two mirror eigen-sectors is plotted in Fig. 2(c), which reveals the nontrivial binding of WCCs and a mirror Chern number of -1. The nontrivial mirror Chern number guarantees the existence of nontrivial Dirac cone states on the surface respecting glide-mirror  $\mathcal{G}_{v_1} = \{\mathcal{M}_{v_1} | \frac{1}{2}\frac{1}{2}0\}$  symmetry. We present the (001) surface band spectrum for Ni-O and La terminated surfaces in Fig. 3. In Figs. 3(a)-3(b), we illustrate the two possible (001) surface terminations that expose the Ni-O

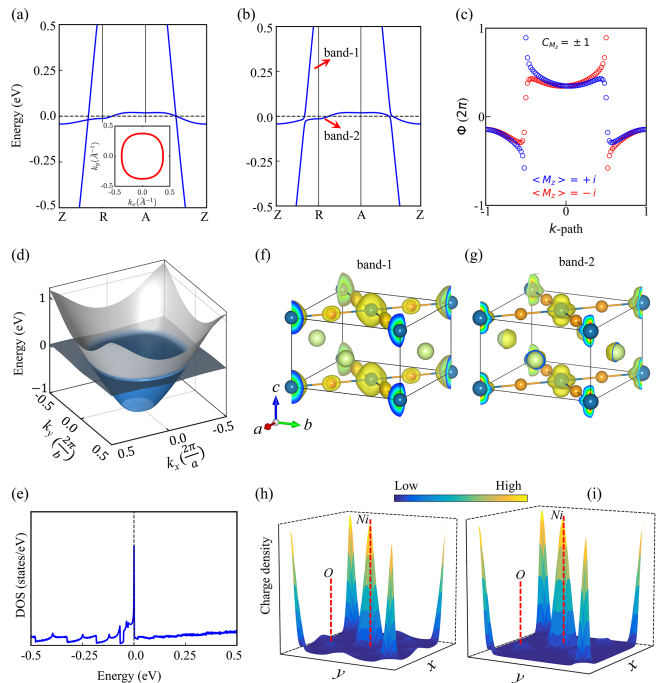


FIG. 2. Closeup of the bulk band structure of  $C$ -AFM phase (a) without and (b) with spin-orbit coupling. Band-1 and band-2 are marked in (b) to facilitate the discussion (see text for details). (c) The evolution of the mirror winding number on the  $k_x = k_y$  plane. The non-zero mirror Chern number shows the TCI phase in the  $C$ -AFM phase of  $\text{LaNiO}_2$ . (d)  $E - k_x - k_y$  plot resolving the crossings band structure on the  $k_z = \pi/c$  plane. (e) Calculated density of states (DOS). A large peaked DOS at the Fermi level highlights VHSs due to the flat band energy. (f)-(g) The charge density associated with band-1 and band-2 represented in the crystal lattice. (h)-(i) The charge density associated with band-1 and band-2 represented in the  $k_z = \pi/c$  plane. A power decay of the Bloch wavefunctions associated with Ni atoms is revealed.

and La atomic planes in the surface layer, respectively. The surface electronic structures associated with the Ni-O and La terminated surfaces are shown in Figs. 3(c)-(e) and 3(f)-3(h), respectively. The clear surface Dirac cone states are seen crossings at the  $\bar{\Gamma}$  point on both the terminations. However, these surface states show distinct energy-momentum dispersion on different terminated surfaces. Specifically, the surface states on the Ni-O surface show a nearly flat energy dispersion with a bandwidth of  $\sim 0.1\text{eV}$  (Figs. 3(c)-3(d)). The surface states overlap with the projected flat bulk bands for the Ni-O surface at the Fermi level in full surface BZ as revealed in the Fermi band contours in Fig. 3(e). In contrast, the surface states on the La terminated surface have a larger bandwidth with a higher group velocity (Figs. 3(f)-3(g)). The associated Fermi band contour in Fig. 3(h) is separated from bulk bands in momentum space. The reason for such a difference in energy dispersion on two terminated surfaces can be attributed to a suppressed hopping strength on Ni-O termination due to

anti-parallel magnetic moments between Ni atoms while there is no such restriction for non-magnetic La termination on the surface.

We turn now to discuss the symmetry protection of the observed surface Dirac fermions. The glide mirror plane  $\mathcal{G}_{v_1} : (x, y, z) \rightarrow (y + \frac{1}{2}, x + \frac{1}{2}, z)$  reflects the states in momentum space at  $(k_x, k_y, k_z)$  to  $(k_y, k_x, k_z)$ . The states on the  $(k_x, k_x, k_z)$  plane can be labeled by glide eigenvalues. To obtain these glide eigenvalues, the relation  $\hat{\mathcal{G}}_{v_1}^2 = \{-E|110\}$  holds for a spin-full system with action on the Bloch states as  $\hat{\mathcal{G}}_{v_1}^2 |\mathbf{k}\rangle = -e^{-i(k_x+k_y)} |\mathbf{k}\rangle$ . Therefore, the glide eigenvalues on the  $(k_x, k_x, k_z)$  plane read as  $g_{\pm} = \pm i e^{-ik_x}$ . In particular, on the line  $k_x = k_y = 0$ , the glide eigenvalues become pure imaginary,  $g_{\pm} = \pm i$ , and the signs are swapped on the line  $k_x = k_y = \pi$ , *i.e.*,  $g_{\pm} = \mp i$ . There could be thus un-avoided band crossing on the surface preserving the glide symmetry ( $\bar{\Gamma} - \bar{M}$  line on (001) surface) as found at  $\bar{\Gamma}$  point in Fig. 3.

Similarly, another vertical glide mirror plane  $\mathcal{G}_{v_2} : (x, y, z) \rightarrow (x + \frac{1}{2}, -y + \frac{1}{2}, z)$  dictates that the states at  $(k_x, k_y, k_z)$  reflects to  $(k_x, -k_y, k_z)$ . The eigenstates on  $k_y = \{0, \pi\}$  planes can be thus labeled by  $\mathcal{G}_{v_2}$  glide eigenvalues. Using the relations  $\hat{\mathcal{G}}_{v_2}^2 = \{-E|110\}$ ,  $\hat{\mathcal{G}}_{v_2}^2 |\mathbf{k}\rangle = -e^{-i(k_x+k_y)} |\mathbf{k}\rangle$ , we obtain  $g_{\pm}(k_x, k_y = 0) = \pm i e^{-ik_x/2}$ ,  $g_{\pm}(k_x, k_y = \pi) = \pm e^{-ik_x/2}$  on the  $k_y = \{0, \pi\}$  planes. On the glide symmetric plane  $k_y = 0$  and for the subspace restricted to the  $k_z$  axis (*i.e.*,  $k_x = 0$ ), the glide eigenvalues become  $g_{\pm} = \pm i$ . This dictates the band degeneracy at  $\bar{\Gamma}$  and thus, the surface states can be gapless along  $\bar{\Gamma} - \bar{X}$  as well. These symmetry properties indicate that the surface Dirac fermions are protected by glide mirror symmetry, and thus, the  $C$ -AFM phase of  $\text{LaNiO}_2$  realizes a symmetry-protected topological crystalline insulator state.

*Possible nontrivial superconducting states.* The preceding analysis demonstrates that  $\text{LaNiO}_2$  is a topological crystalline insulator with nontrivial surface Dirac Fermion states. These states could become superconducting through the bulk proximity effect. We now analyze the possibility of nontrivial superconducting pairing in the bulk states of  $\text{LaNiO}_2$ . Under the glide operation, the symmetric kinetic bulk Hamiltonian transforms as  $\hat{\mathcal{G}}(\mathbf{k})H(\mathbf{k})\hat{\mathcal{G}}(\mathbf{k})^\dagger = H(\mathcal{M}_v\mathbf{k})$ , where  $\hat{\mathcal{G}}(\mathbf{k}) (\equiv \{\mathcal{M}_{v_1/v_2} | \frac{1}{2}\frac{1}{2}0\})$  represents the glide mirror operator in momentum space acting on spin, orbital, and sublattice degrees of freedom. The superconducting model with gap function  $\Delta(\mathbf{k})$  is described by the BdG Hamiltonian,

$$H_{\text{BdG}}(\mathbf{k}) = \begin{pmatrix} H(\mathbf{k}) & \Delta(\mathbf{k}) \\ \Delta^\dagger(\mathbf{k}) & -H^T(-\mathbf{k}) \end{pmatrix}. \quad (2)$$

The bulk symmetries imply that  $\hat{\mathcal{G}}_{\text{BdG}}(\mathbf{k})H_{\text{BdG}}(\mathbf{k})\hat{\mathcal{G}}_{\text{BdG}}(\mathbf{k})^\dagger = H_{\text{BdG}}(\mathcal{M}_v\mathbf{k})$ . Here the symmetry operations are extended to the particle-hole space as  $\hat{\mathcal{G}}_{\text{BdG}}(\mathbf{k}) = \hat{\mathcal{G}}(\mathbf{k}) \oplus [\hat{\mathcal{G}}^\pm(-\mathbf{k})]^*$ . To satisfy this symmetry constraint, the gap function should

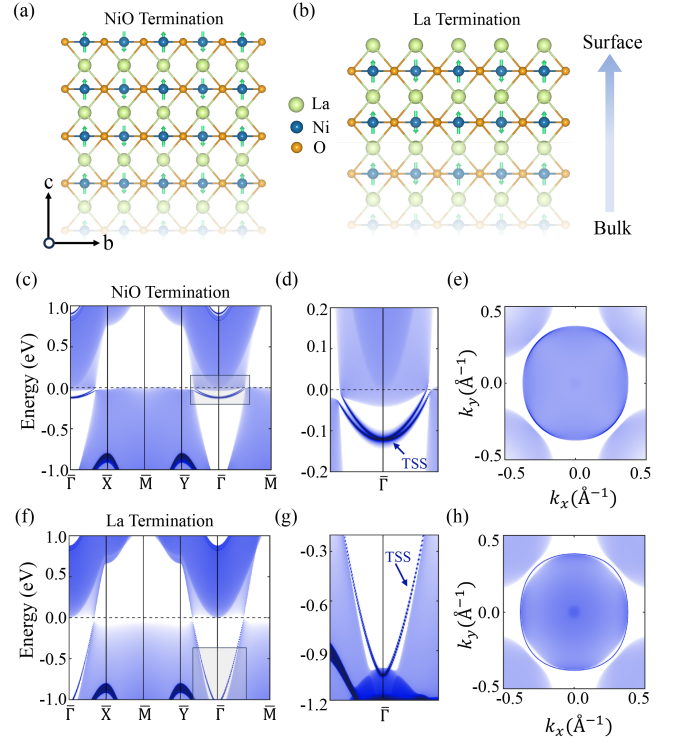


FIG. 3. Lattice structure of a semi-infinite slab of the  $C$ -AFM phase of  $\text{LaNiO}_2$  with (a) NiO and (b) La terminations. (c)-(e) The calculated (001) surface band structure for NiO surface termination (c) with a closeup of surface bands in (d) and associated Fermi band counter in (e). The dark blue color marks the surface states. The horizontal dashed line marks the Fermi level. (f)-(h) Same as (c)-(e) but for La surface termination.

transform as  $\hat{\mathcal{G}}(\mathbf{k})\Delta(\mathbf{k})\hat{\mathcal{G}}^T(-\mathbf{k}) = \pm\Delta(\mathcal{M}_v\mathbf{k})$ . We define  $\hat{\mathcal{G}}^\pm(-\mathbf{k}) = \pm\hat{\mathcal{G}}(-\mathbf{k})$  depending on the even (+) or odd (-) transformation of the gap function under the symmetry operation. For odd-symmetric gap functions, the lattice symmetry operation and particle-hole transformation,  $\hat{\mathcal{C}}H_{\text{BdG}}(\mathbf{k})\hat{\mathcal{C}}^{-1} = -H_{\text{BdG}}(-\mathbf{k})$  should anticommute *i.e.*  $\{\hat{\mathcal{C}}, \hat{\mathcal{G}}\} = 0$ . These symmetry constraints restrict the Hilbert space of Bloch states to one-dimensional lines  $k_x = k_y = 0$  and  $k_x = k_y = \pi$ , which corresponds to  $\bar{\Gamma} - \bar{Z}$  and  $\bar{M} - \bar{A}$  symmetry directions in the bulk BZ, respectively. The Bloch states on these symmetry lines thus acquire pure imaginary glide eigenvalues  $g_{\pm} = \pm i$ :  $\mathcal{H} = \bigoplus_{k_z} (\mathcal{H}_{k_z}^{+i} \oplus \mathcal{H}_{k_z}^{-i})$ .

Let us consider superconducting states with odd-symmetric gap functions. Each eigenvalue sector is preserved under the action of particle-hole symmetry operation due to the anticommutation relation  $\{\hat{\mathcal{C}}, \hat{\mathcal{G}}\} = 0$ , *i.e.*, a glide eigenstate with definite eigenvalue is preserved upon the action of  $\hat{\mathcal{C}}$  [64]. Therefore, each sector is a one-dimensional superconductor that breaks the time-reversal symmetry. It belongs to the  $D$  class of AZ classification. The superconducting states in this class

are characterized by  $\mathbb{Z}_2$  invariant defined as

$$\nu^\pm = \frac{1}{2\pi} \oint A^\pm(k) dk, \quad (3)$$

where  $A^\pm(k) = i \sum_n \langle \psi_n^\pm(k) | \partial_k \psi_n^\pm(k) \rangle$  is the sum of the Berry connection of occupied BdG states with a definite glide eigenvalue, and the integration is over the loops  $Z-\Gamma-Z$  or  $A-M-A$ . For an odd-parity superconductor, the topological invariant is  $\mathbb{Z}_2$  nontrivial and it is shown that the invariant can be deduced from the structure of the Fermi surface of the normal state. The invariant is related to the band structure as [65, 66]:

$$(-1)^{\nu^\pm} = \prod_n \text{sgn} \varepsilon_n^\pm(\Lambda_i) \text{sgn} \varepsilon_n^\pm(\Lambda_j), \quad (4)$$

where  $\varepsilon_n^\pm(\Lambda_i)$  is the eigenstate of the normal Hamiltonian  $H(\mathbf{k})$  at  $\Lambda_i = \Gamma(M)$  and  $\Lambda_j = Z(A)$ . From (4), the invariant is defined modulo 2, and therefore, it can be written as  $(-1)^{\nu^\pm} = (-1)^{p_0} \Rightarrow \nu^\pm = p_0 \pmod{2}$ , where  $p_0$  is the number of times the energy bands with a given glide eigenvalue cross the Fermi level between  $\Lambda_i$  and  $\Lambda_j$ . Using the band structure shown in Figs. 1(e) and 2(b), we give the sign of energy bands crossing the Fermi level in Table I. These results show that  $\mathbb{Z}_2$  invariant,  $\nu^\pm = +1$ , is nontrivial for an odd-parity superconductor. This implies that the surface perpendicular to the  $z$  direction should support zero-energy modes at  $\bar{\Gamma}$ .

As a possible odd-parity pairing candidate, the superconducting state could be a pair-density wave (PDW) with  $B_{2u}$  representation. This irreducible representation allows for  $d$ -wave superconductor,  $k_x^2 - k_y^2$ , within the layers while the sign of the superconducting gap alternates between the layers. A similar PDW state has been proposed as topological crystalline superconductivity in heavy-fermion  $\text{CeRh}_2\text{As}_2$  [64].

TABLE I. Sign of the mirror eigenvalues of energy bands crossing Fermi level at  $\Lambda$  in Fig. 1(e).

$\Lambda$	$\Gamma$	X	M	Z	R	A
$\text{sgn}[\varepsilon(\Lambda)]$	+	+	+	-	-	+

The symmetry of the magnetic state also allows a  $\mathbb{Z}_2$  classification of possible gapped superconducting states in the layered nickelates. The magnetic state breaks both the time-reversal and translational symmetry. Nevertheless, a combination of these operations is preserved in the antiferromagnetic state [67]. We denote the time-reversal operation by  $\Theta$ , and the half-cell translation by  $T_{1/2} \equiv T_{\mathbf{a}/2+\mathbf{b}/2}$ . The combined operation,  $\tilde{\Theta} = \Theta T_{1/2}$ , is the symmetry of the magnetic state. For simplicity, let us define new lattice vectors  $\mathbf{a}_1 = \mathbf{a} + \mathbf{b}$ ,  $\mathbf{a}_2 = \mathbf{a} - \mathbf{b}$  and  $\mathbf{a}_3 = \mathbf{c}$ . The corresponding components of wave vector reads as  $k_1 = \mathbf{k} \cdot \mathbf{a}_1$ ,  $k_2 = \mathbf{k} \cdot \mathbf{a}_2$  and  $k_3 = \mathbf{k} \cdot \mathbf{a}_3$ . In momentum space,  $T_{1/2}^2 = e^{ik_1}$ ,  $\tilde{\Theta}^2 = -e^{ik_1}$ ,

and  $\tilde{\Theta} H_{\text{BdG}}(k_1, k_2, k_3) \tilde{\Theta}^{-1} = H_{\text{BdG}}(-k_1, -k_2, -k_3)$  with  $\Theta^2 = -1$  for spin-1/2 systems. On the plane  $k_1 = 0$  ( $k_x + k_y = 0$ ) or another  $C_4$ -symmetric equivalent plane, *i.e.*, the plane  $k_2 = 0$  for half translation along  $\mathbf{a}_2$ , we have  $\tilde{\Theta}^2 = -1$ . Thus, in analogous to time-reversal invariant insulators, the Hilbert space of Bloch states with gapped spectrum restricted to the plane  $(k_2, k_3)$  can be classified by  $\mathbb{Z}_2$  invariant  $\nu = 1$  ( $\nu = 0$ ) corresponds to topological (trivial) ground state. Note that there is no such classification on the  $k_1 = \pi$  plane since  $\tilde{\Theta}^2 = +1$ . Therefore, the symmetry of the magnetic state allows for a  $\mathbb{Z}_2$  classification of a fully gapped superconductor on the  $(k_2, k_3)$  plane. However, whether the fully gapped superconductor on this plane is topologically nontrivial depends on the details of the band structure of  $H_{\text{BdG}}$ , which constitutes an interesting problem for future studies.

*Conclusion.*— It is widely accepted in the cuprates that the competing inhomogeneous phases and VHSs play a key role in producing their superconducting state. This, however, is not widely discussed in the recently discovered nickelate superconductors despite their similarities with the cuprates. Our in-depth first-principles calculations and symmetry analysis reveal the existence of a flat band in the undoped nickelate superconductor  $\text{LaNiO}_2$ . This flat band mainly involves Ni  $3d_{z^2}$  states and it crosses a hybrid state composed of Ni  $3d_{xz/yz}$  and O  $2p$  orbitals to generate a band inversion in the bulk spectrum. We show that the  $C$ -AFM phase of  $\text{LaNiO}_2$  realizes an axion insulator state with a higher-order invariant  $\mathbb{Z}_4 = 2$  and mirror-symmetry-protected topological crystalline insulator state with nontrivial surface states. We also show that the superconducting state in  $\text{LaNiO}_2$  possesses a nontrivial topological character. Our study not only highlights the similarities between the *undoped* nickelates and the *doped* cuprate superconductors but it also shows that the nickelates would provide an interesting materials platform for exploring the interplay of topological states and nontrivial superconductivity.

## ACKNOWLEDGEMENTS

R.Z. and J.S. acknowledge the support of the U.S. Office of Naval Research (ONR) Grant No. N00014-22-1-2673 and it benefited from NSF's Advanced Cyberinfrastructure Coordination Ecosystem, and the National Energy Research Scientific Computing Center. The work at Northeastern University was supported by the National Science Foundation through NSF-ExpandQISE award #2329067 and it benefited from Northeastern University's Advanced Scientific Computation Center and the Discovery Cluster. The work at TIFR Mumbai was supported by the Department of Atomic Energy of the Government of India under project number 12-R&D-TFR-5.10-0100 and benefited from the computational resources of TIFR Mumbai.

R. Z., C.-Y. H., and M. K. contributed equally to this

work.

- 
- [1] Nicolas Regnault, Yuanfeng Xu, Ming-Rui Li, Da-Shuai Ma, Milena Jovanovic, Ali Yazdani, Stuart S. P. Parkin, Claudia Felser, Leslie M. Schoop, N. Phuan Ong, Robert J. Cava, Luis Elcoro, Zhi-Da Song, and B. Andrei Bernevig, “Catalogue of flat-band stoichiometric materials,” *Nature* **603**, 824–828 (2022).
- [2] Da-Shuai Ma, Yuanfeng Xu, Christie S. Chiu, Nicolas Regnault, Andrew A. Houck, Zhida Song, and B. Andrei Bernevig, “Spin-orbit-induced topological flat bands in line and split graphs of bipartite lattices,” *Physical Review Letters* **125**, 266403 (2020).
- [3] Jia-Xin Yin, Biao Lian, and M. Zahid Hasan, “Topological kagome magnets and superconductors,” *Nature* **612**, 647–657 (2022).
- [4] Evelyn Tang, Jia-Wei Mei, and Xiao-Gang Wen, “High-temperature fractional quantum hall states,” *Phys. Rev. Lett.* **106**, 236802 (2011).
- [5] Kai Sun, Zhengcheng Gu, Hosho Katsura, and S. Das Sarma, “Nearly flatbands with nontrivial topology,” *Phys. Rev. Lett.* **106**, 236803 (2011).
- [6] Yuan Cao, Valla Fatemi, Shiang Fang, Kenji Watanabe, Takashi Taniguchi, Efthimios Kaxiras, and Pablo Jarillo-Herrero, “Unconventional superconductivity in magic-angle graphene superlattices,” *Nature* **556**, 43–50 (2018).
- [7] Rafi Bistritzer and Allan H. MacDonald, “Moiré bands in twisted double-layer graphene,” *Proceedings of the National Academy of Sciences* **108**, 12233–12237 (2011).
- [8] Hui Chen, Haitao Yang, Bin Hu, Zhen Zhao, Jie Yuan, Yuqing Xing, Guojian Qian, Zihao Huang, Geng Li, Yuhua Ye, Sheng Ma, Shunli Ni, Hua Zhang, Qiangwei Yin, Chunsheng Gong, Zhijun Tu, Hechang Lei, Hengxin Tan, Sen Zhou, Chengmin Shen, Xiaoli Dong, Binghai Yan, Ziqiang Wang, and Hong-Jun Gao, “Roton pair density wave in a strong-coupling kagome superconductor,” *Nature* **599**, 222–228 (2021).
- [9] Mingu Kang, Shiang Fang, Jonggyu Yoo, Brenden R. Ortiz, Yuzki M. Oey, Jonghyeok Choi, Sae Hee Ryu, Jimin Kim, Chris Jozwiak, Aaron Bostwick, Eli Rotenberg, Efthimios Kaxiras, Joseph G. Checkelsky, Stephen D. Wilson, Jae-Hoon Park, and Riccardo Comin, “Charge order landscape and competition with superconductivity in kagome metals,” *Nature Materials* **22**, 186–193 (2022).
- [10] Zhicheng Jiang, Zhengtai Liu, Haiyang Ma, Wei Xia, Zhonghao Liu, Jishan Liu, Soohyun Cho, Yichen Yang, Jianyang Ding, Jiayu Liu, Zhe Huang, Yuxi Qiao, Jijia Shen, Wenchuan Jing, Xiangqi Liu, Jianpeng Liu, Yanfeng Guo, and Dawei Shen, “Flat bands, non-trivial band topology and rotation symmetry breaking in layered kagome-lattice  $\text{rbt}3\text{bi}5$ ,” *Nature Communications* **14**, 4892 (2023).
- [11] Bahadur Singh, “Rotation rearranges electrons,” *Nature Physics* (2023), 10.1038/s41567-023-02237-7.
- [12] Yaojia Wang, Heng Wu, Gregory T. McCandless, Julia Y. Chan, and Mazhar N. Ali, “Quantum states and intertwining phases in kagome materials,” *Nature Reviews Physics* (2023), 10.1038/s42254-023-00635-7.
- [13] Mingu Kang, Shiang Fang, Linda Ye, Hoi Chun Po, Jonathan Denlinger, Chris Jozwiak, Aaron Bostwick, Eli Rotenberg, Efthimios Kaxiras, Joseph G. Checkelsky, and Riccardo Comin, “Topological flat bands in frustrated kagome lattice  $\text{CoSn}$ ,” *Nature Communications* **11**, 1–9 (2020).
- [14] Robert S. Markiewicz, Bahadur Singh, Christopher Lane, and Arun Bansil, “Investigating the cuprates as a platform for high-order van Hove singularities and flat-band physics,” *Communications Physics* **6**, 292 (2023).
- [15] Danfeng Li, Kyuho Lee, Bai Yang Wang, Motoki Osada, Samuel Crossley, Hye Ryoung Lee, Yi Cui, Yasuyuki Hikita, and Harold Y. Hwang, “Superconductivity in an infinite-layer nickelate,” *Nature* **572**, 624–627 (2019).
- [16] Motoki Osada, Bai Yang Wang, Berit H. Goodge, Kyuho Lee, Hyeok Yoon, Keita Sakuma, Danfeng Li, Masashi Miura, Lena F. Kourkoutis, and Harold Y. Hwang, “A Superconducting Praseodymium Nickelate with Infinite Layer Structure,” *Nano Letters* **20**, 5735–5740 (2020).
- [17] Shengwei Zeng, Changjian Li, Lin Er Chow, Yu Cao, Zhaoting Zhang, Chi Sin Tang, Xinmao Yin, Zhi Shih Lim, Junxiong Hu, Ping Yang, and Ariando Ariando, “Superconductivity in infinite-layer nickelate  $\text{la}_{1-x}\text{ca}_x\text{nio}_2$  thin films,” *Science Advances* **8**, 9927 (2022).
- [18] Motoki Osada, Bai Yang Wang, Berit H. Goodge, Shannon P. Harvey, Kyuho Lee, Danfeng Li, Lena F. Kourkoutis, and Harold Y. Hwang, “Nickelate Superconductivity without Rare-Earth Magnetism:  $(\text{La},\text{Sr})\text{NiO}_2$ ,” *Advanced Materials* **33** (2021), 10.1002/adma.202104083.
- [19] George A. Sawatzky, “Superconductivity seen in a non-magnetic nickel oxide,” *Nature* **572**, 592–593 (2019).
- [20] Michael R. Norman, “Entering the Nickel Age of Superconductivity,” *Physics* **13**, 85 (2020).
- [21] Warren E. Pickett, “The dawn of the nickel age of superconductivity,” *Nature Reviews Physics* **3**, 7–8 (2021).
- [22] M. Hepting, D. Li, C. J. Jia, H. Lu, E. Paris, Y. Tseng, X. Feng, M. Osada, E. Been, Y. Hikita, Y.-D. Chuang, Z. Hussain, K. J. Zhou, A. Nag, M. Garcia-Fernandez, M. Rossi, H. Y. Huang, D. J. Huang, Z. X. Shen, T. Schmitt, H. Y. Hwang, B. Moritz, J. Zaanen, T. P. Devereaux, and W. S. Lee, “Electronic structure of the parent compound of superconducting infinite-layer nickelates,” *Nature Materials* **19**, 381–385 (2020).
- [23] Zhao Liu, Zhi Ren, Wei Zhu, Zhengfei Wang, and Jinlong Yang, “Electronic and magnetic structure of infinite-layer  $\text{NdNiO}_2$ : trace of antiferromagnetic metal,” *npj Quantum Materials* **5**, 31 (2020).
- [24] Mi Young Choi, Kwan Woo Lee, and Warren E. Pickett, “Role of 4f states in infinite-layer  $\text{NdNiO}_2$ ,” *Physical Review B* **101**, 20503 (2020).
- [25] Peiheng Jiang, Liang Si, Zhaoliang Liao, and Zhicheng Zhong, “Electronic structure of rare-earth infinite-layer  $r\text{NiO}_2$  ( $r = \text{La}, \text{Nd}$ ),” *Phys. Rev. B* **100**, 201106 (2019).
- [26] Frank Lechermann, “Late transition metal oxides with infinite-layer structure: Nickelates versus cuprates,” *Physical Review B* **101**, 081110 (2020), 1911.11521.
- [27] I. Leonov, S. L. Skornyakov, and S. Y. Savrasov, “Lifshitz transition and frustration of magnetic moments in infinite-layer  $\text{ndnio}_2$  upon hole doping,” *Phys. Rev. B*

- 101**, 241108 (2020).
- [28] K.-W. Lee and W. E. Pickett, “Infinite-layer  $\text{LaNiO}_2$ :  $\text{ni}^{1+}$  is not  $\text{cu}^{2+}$ ,” *Phys. Rev. B* **70**, 165109 (2004).
- [29] Danfeng Li, Bai Yang Wang, Kyuho Lee, Shannon P. Harvey, Motoki Osada, Berit H. Goodge, Lena F. Kourkoutis, and Harold Y. Hwang, “Superconducting dome in  $\text{Nd}_{1-x}\text{Sr}_x\text{NiO}_2$  infinite layer films,” *Phys. Rev. Lett.* **125**, 027001 (2020).
- [30] Hirofumi Sakakibara, Hidetomo Usui, Katsuhiko Suzuki, Takao Kotani, Hideo Aoki, and Kazuhiko Kuroki, “Model construction and a possibility of cupratelike pairing in a new  $d^9$  nickelate superconductor  $(\text{Nd}, \text{Sr})\text{NiO}_2$ ,” *Phys. Rev. Lett.* **125**, 077003 (2020).
- [31] A. S. Botana and M. R. Norman, “Similarities and differences between  $\text{LaNiO}_2$  and  $\text{CaCuO}_2$  and implications for superconductivity,” *Phys. Rev. X* **10**, 011024 (2020).
- [32] Jonathan Karp, Antia S. Botana, Michael R. Norman, Hyowon Park, Manuel Zingl, and Andrew Millis, “Many-body electronic structure of  $\text{NdNiO}_2$  and  $\text{CaCuO}_2$ ,” *Phys. Rev. X* **10**, 021061 (2020).
- [33] Berit H. Goodge, Danfeng Li, Kyuho Lee, Motoki Osada, Bai Yang Wang, George A. Sawatzky, Harold Y. Hwang, and Lena F. Kourkoutis, “Doping evolution of the Mott–Hubbard landscape in infinite-layer nickelates,” *Proceedings of the National Academy of Sciences* **118**, e2007683118 (2021).
- [34] Mi Jiang, Mona Berciu, and George A. Sawatzky, “Critical Nature of the Ni Spin State in Doped  $\text{NdNiO}_2$ ,” *Phys. Rev. Lett.* **124**, 207004 (2020).
- [35] Ruiqi Zhang, Christopher Lane, Bahadur Singh, Johannes Nokelainen, Bernardo Barbiellini, Robert S. Markiewicz, Arun Bansil, and Jianwei Sun, “Magnetic and f-electron effects in  $\text{LaNiO}_2$  and  $\text{NdNiO}_2$  nickelates with cuprate-like  $3d_{x^2-y^2}$  band,” *Communications Physics* **4**, 118 (2021).
- [36] Ruiqi Zhang, Christopher Lane, Johannes Nokelainen, Bahadur Singh, Bernardo Barbiellini, Robert S. Markiewicz, Arun Bansil, and Jianwei Sun, “Peierls distortion driven multi-orbital origin of charge density waves in the undoped infinite-layer nickelate,” *arXiv e-prints* (2022), 10.48550/arXiv.2207.00184.
- [37] Christopher Lane, Ruiqi Zhang, Bernardo Barbiellini, Robert S. Markiewicz, Arun Bansil, Jianwei Sun, and Jian-Xin Zhu, “Competing incommensurate spin fluctuations and magnetic excitations in infinite-layer nickelate superconductors,” *Communications Physics* **6**, 90 (2023).
- [38] Matteo Rossi, Motoki Osada, Jaewon Choi, Stefano Agrestini, Daniel Jost, Yonghun Lee, Haiyu Lu, Bai Yang Wang, Kyuho Lee, Abhishek Nag, Yi-De Chuang, Cheng-Tai Kuo, Sang-Jun Lee, Brian Moritz, Thomas P. Devereaux, Zhi-Xun Shen, Jun-Sik Lee, Ke-Jin Zhou, Harold Y. Hwang, and Wei-Sheng Lee, “A broken translational symmetry state in an infinite-layer nickelate,” *Nat. Phys.* **18**, 869–873 (2022).
- [39] G. Krieger, L. Martinelli, S. Zeng, L. E. Chow, K. Kummer, R. Arpaia, M. Moretti Sala, N. B. Brookes, A. Ariando, N. Viart, M. Salluzzo, G. Ghiringhelli, and D. Preziosi, “Charge and spin order dichotomy in  $\text{NdNiO}_2$  driven by the capping layer,” *Phys. Rev. Lett.* **129**, 027002 (2022).
- [40] Charles C. Tam, Jaewon Choi, Xiang Ding, Stefano Agrestini, Abhishek Nag, Mei Wu, Bing Huang, Huiqian Luo, Peng Gao, Mirian García-Fernández, Liang Qiao, and Ke-Jin Zhou, “Charge density waves in infinite-layer  $\text{NdNiO}_2$  nickelates,” *Nat. Mater.* **21**, 1116–1120 (2022), 2112.04440.
- [41] Motoki Osada, Bai Yang Wang, Berit H. Goodge, Shannon P. Harvey, Kyuho Lee, Danfeng Li, Lena F. Kourkoutis, and Harold Y. Hwang, “Nickelate superconductivity without rare-earth magnetism:  $(\text{La}, \text{Sr})\text{NiO}_2$ ,” *Advanced Materials* **33**, 2104083 (2021).
- [42] Jennifer Fowlie, Marios Hadjimichael, Maria M. Martins, Danfeng Li, Motoki Osada, Bai Yang Wang, Kyuho Lee, Yonghun Lee, Zaher Salman, Thomas Prokscha, Jean-Marc Triscone, Harold Y. Hwang, and Andreas Suter, “Intrinsic magnetism in superconducting infinite-layer nickelates,” *Nat. Phys.* **18**, 1043–1047 (2022).
- [43] H. Lu, M. Rossi, A. Nag, M. Osada, D. F. Li, K. Lee, B. Y. Wang, M. Garcia-Fernandez, S. Agrestini, Z. X. Shen, E. M. Been, B. Moritz, T. P. Devereaux, J. Zaanen, H. Y. Hwang, Ke-Jin Zhou, and W. S. Lee, “Magnetic excitations in infinite-layer nickelates,” *Science* **373**, 213–216 (2021).
- [44] R. A. Ortiz, P. Puphal, M. Klett, F. Hotz, R. K. Kremer, H. Trepka, M. Hemmida, H. A. Krug von Nidda, M. Isobe, R. Khasanov, H. Luetkens, P. Hansmann, B. Keimer, T. Schäfer, and M. Hepting, “Magnetic correlations in infinite-layer nickelates: an experimental and theoretical multi-method study,” *arXiv e-prints*, arXiv:2111.13668 (2021), arXiv:2111.13668 [cond-mat.str-el].
- [45] Yuhao Gu, Sichen Zhu, Xiaoxuan Wang, Jiangping Hu, and Hanghui Chen, “A substantial hybridization between correlated Ni-d orbital and itinerant electrons in infinite-layer nickelates,” *Communications Physics* **3**, 84 (2020).
- [46] Motoharu Kitatani, Liang Si, Oleg Janson, Ryotaro Arita, Zhicheng Zhong, and Karsten Held, “Nickelate superconductors—a renaissance of the one-band Hubbard model,” *npj Quantum Materials* **5**, 59 (2020).
- [47] L. E. Chow, S. Kunniniyil Sudheesh, Z. Y. Luo, P. Nandi, T. Heil, J. Deuschle, S. W. Zeng, Z. T. Zhang, S. Prakash, X. M. Du, Z. S. Lim, Peter A. van Aken, Elbert E. M. Chia, and A. Ariando, “Pairing symmetry in infinite-layer nickelate superconductor,” *arXiv e-prints*, arXiv:2201.10038 (2022), arXiv:2201.10038 [cond-mat.supr-con].
- [48] Andreas Kreisel, Brian M. Andersen, Astrid T. Rømer, Ilya M. Eremin, and Frank Lechermann, “Superconducting instabilities in strongly correlated infinite-layer nickelates,” *Phys. Rev. Lett.* **129**, 077002 (2022).
- [49] Jiacheng Gao, Shiyu Peng, Zhijun Wang, Chen Fang, and Hongming Weng, “Electronic structures and topological properties in nickelates  $\text{Ln}_{n+1}\text{Ni}_n\text{O}_{2n+2}$ ,” *National Science Review* **8** (2020).
- [50] Mi-Young Choi, Warren E. Pickett, and Kwan-Woo Lee, “Fluctuation-frustrated flat band instabilities in  $\text{NdNiO}_2$ ,” *Phys. Rev. Research* **2**, 033445 (2020).
- [51] G. Kresse and D. Joubert, “From ultrasoft pseudopotentials to the projector augmented-wave method,” *Physical Review B* **59**, 1758–1775 (1999).
- [52] G. Kresse and J. Hafner, “Ab initio molecular dynamics for open-shell transition metals,” *Physical Review B* **48**, 13115–13118 (1993).
- [53] G. Kresse and J. Furthmüller, “Efficient iterative schemes for ab initio total-energy calculations using a plane-wave basis set,” *Physical Review B* **54**, 11169–11186 (1996).
- [54] Jianwei Sun, Adrienn Ruzsinszky, and Johnp Perdew, “Strongly Constrained and Appropriately Normed

- Semilocal Density Functional,” *Physical Review Letters* **115**, 036402 (2015).
- [55] Yubo Zhang, Christopher Lane, James W. Furness, Bernardo Barbiellini, John P. Perdew, Robert S. Markiewicz, Arun Bansil, and Jianwei Sun, “Competing stripe and magnetic phases in the cuprates from first principles,” *Proceedings of the National Academy of Sciences* **117**, 68–72 (2020).
- [56] James W. Furness, Yubo Zhang, Christopher Lane, Ioana Gianina Buda, Bernardo Barbiellini, Robert S. Markiewicz, Arun Bansil, and Jianwei Sun, “An accurate first-principles treatment of doping-dependent electronic structure of high-temperature cuprate superconductors,” *Communications Physics* **1**, 11 (2018).
- [57] Christopher Lane, James W. Furness, Ioana Gianina Buda, Yubo Zhang, Robert S. Markiewicz, Bernardo Barbiellini, Jianwei Sun, and Arun Bansil, “Antiferromagnetic ground state of  $\text{La}_2\text{CuO}_4$  : A parameter-free *ab-initio* description,” *Physical Review B* **98**, 125140 (2018).
- [58] Yubo Zhang, James Furness, Ruiqi Zhang, Zhi Wang, Alex Zunger, and Jianwei Sun, “Symmetry-breaking polymorphous descriptions for correlated materials without interelectronic  $u$ ,” *Phys. Rev. B* **102**, 045112 (2020).
- [59] Ruiqi Zhang, Bahadur Singh, Christopher Lane, Jamin Kidd, Yubo Zhang, Bernardo Barbiellini, Robert S. Markiewicz, Arun Bansil, and Jianwei Sun, “Critical role of magnetic moments in heavy-fermion materials: Revisiting  $\text{smb}_6$ ,” *Phys. Rev. B* **105**, 195134 (2022).
- [60] Arash A. Mostofi, Jonathan R. Yates, Giovanni Pizzi, Young-Su Lee, Ivo Souza, David Vanderbilt, and Nicola Marzari, “An updated version of wannier90: A tool for obtaining maximally-localised wannier functions,” *Computer Physics Communications* **185**, 2309–2310 (2014).
- [61] F. Guinea, C. Tejedor, F. Flores, and E. Louis, “Effective two-dimensional hamiltonian at surfaces,” *Phys. Rev. B* **28**, 4397–4402 (1983).
- [62] MP Lopez Sancho, JM Lopez Sancho, and Jessy Rubio, “Quick iterative scheme for the calculation of transfer matrices: application to  $\text{mo}(100)$ ,” *J. Phys. F: Met. Phys* **14**, 1205 (1984).
- [63] Yuanfeng Xu, Zhida Song, Zhijun Wang, Hongming Weng, and Xi Dai, “Higher-order topology of the axion insulator  $\text{euin}_2\text{as}_2$ ,” *Phys. Rev. Lett.* **122**, 256402 (2019).
- [64] Kosuke Nogaki, Akito Daido, Jun Ishizuka, and Youichi Yanase, “Topological crystalline superconductivity in locally noncentrosymmetric  $\text{cerh}_2\text{as}_2$ ,” *Phys. Rev. Res.* **3**, L032071 (2021).
- [65] Liang Fu and Erez Berg, “Odd-parity topological superconductors: Theory and application to  $\text{cu}_x\text{bi}_2\text{se}_3$ ,” *Phys. Rev. Lett.* **105**, 097001 (2010).
- [66] Masatoshi Sato, “Topological odd-parity superconductors,” *Phys. Rev. B* **81**, 220504 (2010).
- [67] Roger S. K. Mong, Andrew M. Essin, and Joel E. Moore, “Antiferromagnetic topological insulators,” *Phys. Rev. B* **81**, 245209 (2010).